Time Scales of Terrestrial Carbon Response Related to Land-Use Application: Implications for Initializing an Earth System Model

Lori T. Sentman*

Geophysical Fluid Dynamics Laboratory, NOAA, Princeton, New Jersey

Elena Shevliakova

Department of Ecology and Evolutionary Biology, Princeton University, Princeton, New Jersey

Ronald J. Stouffer

Geophysical Fluid Dynamics Laboratory, NOAA, Princeton, New Jersey

Sergey Malyshev

Department of Ecology and Evolutionary Biology, Princeton University, Princeton, New Jersey

Received 25 January 2011; accepted 18 June 2011

ABSTRACT: The dynamic vegetation and carbon cycling component, LM3V, of the Geophysical Fluid Dynamics Laboratory (GFDL) prototype Earth system model (ESM2.1), has been designed to simulate the effects of land use on terrestrial carbon pools, including secondary vegetation regrowth. Because

* Corresponding author address: Lori T. Sentman, Geophysical Fluid Dynamics Laboratory, NOAA, Princeton University, Forrestal Campus, 201 Forrestal Road, Princeton, NJ 08540-6649, Tel: (609) 452-6563, Fax: (609) 987-5063.
E-mail address: lori.sentman@noaa.gov

DOI: 10.1175/2011EI401.1

of the long time scales associated with the carbon adjustment, special consideration is required when initializing the ESM when historical simulations are conducted. Starting from an equilibrated, preindustrial climate and potential vegetation state in an offline land-only model (LM3V), estimates of historical land use are instantaneously applied in five experiments beginning in the following calendar years: 1500, 1600, 1700, 1750, and 1800. This application results in the land carbon pools experiencing an abrupt change—a carbon shock—and the secondary vegetation needs time to regrow into consistency with the harvesting history. The authors find that it takes approximately 100 years for the vegetation to recover from the carbon shock, whereas soils take at least 150 years to recover. The vegetation carbon response is driven primarily by land-use history, whereas the soil carbon response is affected by both land-use history and the geographic pattern of soil respiration rates. Based on these results, the authors recommend the application of historical land-use scenarios in 1700 to provide sufficient time for the land carbon in ESMs with secondary vegetation to equilibrate to adequately simulate carbon stores at the start of the historical integrations (i.e., 1860) in a computationally efficient manner.

KEYWORDS: Terrestrial carbon; Land use

1. Introduction

The terrestrial biosphere is an important component of the global carbon cycle and actively exchanges carbon with the atmosphere on varying time scales. Conversion of natural lands for agriculture and wood harvesting has shaped the land surface for centuries. Hurtt et al. (Hurtt et al. 2006) found that 42%–68% of the global land surface was altered by anthropogenic land-use activities between 1700 and 2000. Pongratz et al. (Pongratz et al. 2009) showed that anthropogenic land-cover change significantly disturbed the state of the carbon cycle by 1850, when present and future climate–carbon cycle studies typically begin. The Intergovernmental Panel on Climate Change (IPCC) Fourth Assessment Report (AR4) (Denman et al. 2007) suggested considerable uncertainty about the magnitude of the carbon fluxes into the atmosphere resulting from historical land use. Previous estimates of the global and regional net land-use carbon flux for the 1980s and 1990s have been obtained from either bookkeeping models (Houghton 1999; Houghton 2003; DeFries et al. 2002) or process-based models (McGuire et al. 2001; Jain and Yang 2005; Shevliakova et al. 2009). The most recent bookkeeping estimates from Houghton (Houghton 2008) suggest that the global terrestrial biosphere was a net source of 148.6 GtC to the atmosphere between 1850 and 2000 resulting from changes in land use. This estimate is 7.4 GtC smaller than a previous bookkeeping estimate (Houghton 2003), primarily because of lower estimates of tropical deforestation during the 1990s.

Studies investigating the imbalance between estimates from inverse models and observations, known as a missing carbon sink, have attributed the mechanism responsible for the sink to terrestrial processes, such as the enhanced growth due to CO_2 and N fertilization (Canadell et al. 2007), whereas other studies focused on the role of vegetation regrowth (secondary vegetation) following disturbances such as logging or deforestation. Hurtt et al. (Hurtt et al. 2006) found that, in neglecting land-use activities (e.g., wood harvesting and shifting cultivation), the area of secondary vegetation was underestimated by 70%–90% by 2000. Estimates

obtained from Pacala et al. (Pacala et al. 2001) showed that secondary vegetation regrowth increased the carbon sink in the coterminous United States by approximately 0.12–0.13 GtC yr^{-1}. Shevliakova et al. (Shevliakova et al. 2009) suggested a tropical secondary vegetation sink, which in turn reduced the land-use source to 1.1–1.3 GtC yr^{-1} in the 1990s. To better ascertain the mechanisms and impacts of land-use change on the global carbon cycle, research involving more comprehensive historical land-use data and simulations of the fully interactive carbon cycle are needed.

Earth system models (ESMs) are tools specifically designed to further understand the feedbacks and interactions of Earth's biogeochemical cycles among its components. Of particular interest is the simulation of the carbon cycle. A large part of the Coupled Model Intercomparison Project phase 5 (CMIP5) and the IPCC AR5 assessment will be made using the new ESMs. The National Oceanic and Atmospheric Administration (NOAA)/Geophysical Fluid Dynamics Laboratory (GFDL) ESMs are designed to apply scenarios of land use in the form of annual transition rates among the four categories: natural, secondary, croplands, and pastures. Transition rates from 1500 to 2005 are obtained from the Global Land-Use Model (GLM) (Hurtt et al. 2006; Chini et al. 2008). This design allows the land component of the GFDL ESMs to simulate a fully interactive carbon cycle based on historical information about land-use activities and patterns such as wood harvesting and shifting cultivation. The GFDL ESMs are among very few of the AR5-class ESMs that are capable of simulating the historical and secondary vegetation age structure (Shevliakova et al. 2009). Realistic representation of carbon storage in secondary vegetation is an important factor in determining the magnitude of terrestrial carbon uptake of atmospheric CO_2 and thus net terrestrial carbon flux to the atmosphere (Pacala et al. 2001).

The CMIP5 (http://cmip-pcmdi.llnl.gov/cmip5/) experimental design (Taylor et al. 2011, manuscript submitted to *Bull. Amer. Meteor. Soc.*) includes simulations where the climate system is subjected to observed forcings or perturbations from the preindustrial period (at GFDL typically beginning in 1860) to 2005 and into the future. The preindustrial to present day experiments are called historical or twentieth-century simulations (Randall et al. 2007). The GLM land-use scenario (Chini et al. 2008) is one of the forcings applied to the GFDL ESMs in these historical simulations. The historical land-use scenarios are the first global, gridded estimates of the patterns of land use (Hurtt et al. 2006).

In the GFDL ESMs, the historical simulations are initialized in 1860 from a physical integration using constant 1860 radiative forcing and a land state consistent with the prior land-use history (Figure 1) derived by instantaneously applying the pre-1860 land-use history to the equilibrium ''potential'' vegetation land state (all natural) simulated in the 1860 control integration also using constant 1860 radiative forcing. When a historical land-use scenario is instantaneously applied to the 1860 control climate integration, several issues arise. The land and atmosphere system experience an abrupt change in carbon stocks, a carbon shock, as the land undergoes a transition from the potential vegetation state to the historically integrated state prescribed by the GLM scenario at that particular time. The instantaneous cutting of natural forests (i.e., potential vegetation) results in a drastic change in the carbon stocks through deforestation and logging. First, following wood harvesting, the secondary (at least once cut/harvested) vegetation needs time

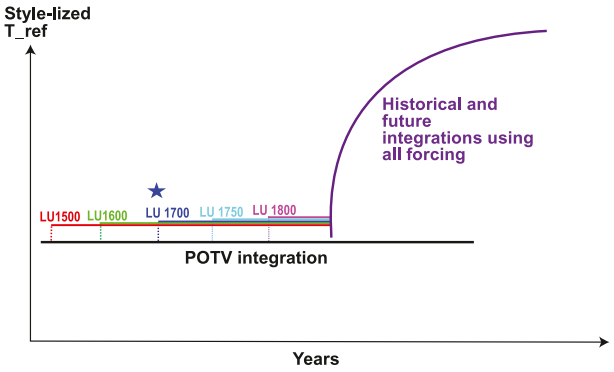

Figure 1. Schematic of experimental design for integrating a historical experiment using GFDL's ESM. The black line represents the global surface air temperature in the POTV integration. The purple line represents the global surface air temperatures in the historical and future integrations. The five lines (red for LU1500, green for LU1600, blue for LU1700, cyan for LU1750 and magenta for LU1800) represent the global surface air temperatures in the integration started from the POTV integration, where only the historical land-use changes are applied for the five land-use experiments with the same climate in this paper. The blue line and star represent the global surface air temperatures in the integration started from the POTV integration, where only the historical land-use changes are applied starting in 1700 for the GFDL ESMs for CMIP5 and IPCC AR5.

to regrow, which is essential for producing the appropriate time history of terrestrial carbon stores and fluxes. Second, when land use is introduced in the model, the transition rates are accumulated from the beginning of the dataset (1500). Therefore, even in the absence of wood harvesting, the scenario's initial rate of deforestation could be higher than a typical annual rate and this could imply a sudden, drastic increase in the soil carbon pools. Third, at the time of the initial, historical land-use application, a large amount of carbon is released into the atmosphere. If these abrupt changes occur at 1860, the historical integration will be unduly affected by the carbon shock of the additional carbon in the atmosphere.

The issues above apply to any ESM's land component simulating harvesting and deforestation. It raises the question of how far before the start of the historical integration (i.e., 1860) the initial application of land use needs to begin to allow the secondary vegetation and soil carbon pools to adjust in order to produce realistic terrestrial carbon stores and fluxes by 1860 (the start of the historical integration). Land use could be applied to the potential vegetation state in the control integration when the GLM scenarios begin in 1500 or anytime thereafter. However, running an ESM from 1500 to 1860 with historical land-use scenarios would greatly increase the computational requirements for the experiments. For example, ESM2.1 using about 230 processors on our computer system at GFDL realizes about 10 model years per calendar day when the model is running continuously. Integrating the period 1500–1860 would take about 36 calendar days and is a substantial cost. In this paper, we present an analysis of the simulated land carbon response to

the timing of the initial application of historical land-use scenarios and provide a computationally efficient approach for initializing land-use states in any ESM historical simulations incorporating secondary forest regrowth and deforestation.

2. Model description

Only a brief description of the land carbon model is given here. Shevliakova et al. (Shevliakova et al. 2009) provide a more detailed description of the model and of the carbon redistribution following land use.

In LM3V, carbon is stored in three main reservoirs: vegetation, soil, and anthropogenic (Shevliakova et al. 2009). Vegetation carbon is represented by five pools: leaves, fine roots, sapwood, labile carbon stores, and wood. The living carbon pool includes all vegetation carbon pools but wood. Carbon is allowed to change in the living carbon pools daily and is a function of net primary production (NPP), phenological and mortality losses, and harvesting. Wood carbon changes depend on the conversion of sapwood into wood and mortality. Soil carbon is stored in two pools characterized by the fast and slow decomposition rates of Bolker et al. (Bolker et al. 1998). The anthropogenic carbon pool includes transfers of carbon from vegetation following the harvesting of carbon on agricultural lands, land clearing, and logging, and it is accompanied by deposition of residue into the soil pools.

The LM3V model simulates the fraction of land occupied by four land-use types: croplands, pasture, secondary and natural vegetation, and the associated carbon pools. Each grid cell in LM3V is made up of a combination of tiles representing land use at that particular location. Historical transition rates of land use are applied in LM3V at the end of each model year, and carbon is reallocated among the terrestrial pools depending on the type of transition. For example, when natural or secondary forests are harvested for wood, 75% of the biomass is assumed to be deposited into the anthropogenic carbon pool. The remaining 25% is assumed to remain on site and is deposited into the soil carbon pool.

3. Experiment design

To investigate the effect of the timing of historical land-use application on the terrestrial carbon, six experiments were performed using the stand-alone version of LM3V forced with 3-hourly climate variables obtained from a prior 1860 atmosphere–ocean general circulation model (AOGCM) control climate integration of the GFDL Climate Model version 2.0 (CM2.1) (Delworth et al. 2006). The AOGCM provided 50 years of data that were used repeatedly in the six experiments discussed here, allowing decadal climate variability. In all experiments, the photosynthesis CO_2 levels were prescribed at the 1860 level (286 ppm).

The first experiment was a 400-yr spinup integration under the assumption of no land-use activities. This experiment yielded the distribution of vegetation and soil carbon stores for potential vegetation under 1860 climate conditions (referred to as the POTV integration). Potential vegetation was used in the spinup integration to obtain a near-equilibrium terrestrial carbon state that could not be achieved with land use for two reasons: the terrestrial carbon is constantly adjusting as land-use forcing is applied, and the resulting response in the carbon stores to land use is also

time dependent given a time-invariant land-use application. Therefore, the only method to achieve an equilibrium carbon state is to integrate the model without land use (i.e., a potential vegetation state). Because equilibration of soil carbon can take thousands of years (Kucharik et al. 2000; Hoffman et al. 2005), the equilibrium soil carbon values were analytically estimated (Shevliakova et al. 2009) in a separate step after 250 years of the POTV experiment. The equilibrium carbon state from the POTV experiment was established when the drift in carbon stocks was less than 2% per 350 years, and the POTV experiment was used to initialize five other experiments with different assumptions about the timing of the initial application of historical land-use scenarios. The historical land-use transition rates (Chini et al. 2008) were imposed on the POTV integration starting from different calendar years: 1500, 1600, 1700, 1750, and 1800. These form five new experiments, LU1500, LU1600, LU1700, LU1750, and LU1800.

The cumulative, historical land-use transition rates were preserved at the start of each land-use experiment so that all experiments had the same fractions of croplands, pastures, and secondary forest in each grid cell in the same calendar year. The historical land-use transition rates were accumulated from 1500 to the time when the initial land-use transitions were applied in the model. For example, when land use was imposed on the potential vegetation state in the LU1700 experiment, the cumulative, historical land-use transition rates from 1500 to 1700 were instantaneously introduced in the model at the end of year 1700. Although the total secondary fraction was preserved, the information about age distribution and number of secondary tiles was lost computing the initial, accumulated transition rates to secondary vegetation. Although GFDL AOGCMs and ESMs typically simulate 1860 control and start historical integrations using 1860 initial conditions, the five land-use experiments in this study were integrated until 1850 and the terrestrial carbon was analyzed at 50-yr intervals between 1500 and 1850. Because LU1500 was the longest land-use integration (350 simulated years) in this study and the historical land-use dataset provides no information about land-use transitions before 1500, LU1500 is considered the target simulation. The other four land-use experiments were compared to the target experiment in order to determine the sensitivity of the carbon stocks and fluxes to the historical land-use transitions initiated at a later date (i.e., 1600, 1700, 1750, and 1800).

4. Results

4.1. Changes in land-use patterns prior to the 1860s

Land-use practices have significantly altered the state of the land surface for centuries prior to the 1860s. According to the historical land-use scenario, by 1500, 3.7% (4.9×10^6 km^2) of land surface was converted for agricultural use. By 1700, 14.2% (18.9×10^6 km^2) of land was impacted by human management. In 1850, 22.2% (29.7×10^6 km^2) of land was either converted for agriculture or was in a state of recovery (secondary forest regrowth). From 1500 to 1850, although the area of primary vegetation decreased, the areas of crops, pastures, and secondary vegetation increased to 5.7×10^6 km^2, 7.9×10^6 km^2, and 16.1×10^6 km^2, respectively (Table 1). Primary vegetation area decreased rapidly in the last 50 years of the simulation (−3.5% from 1800 to 1850) compared to earlier periods

Table 1. Global total land area (10^6 km^2) occupied by land-use types. Numbers in parentheses indicate global percent (%) of total land area occupied by each land-use type.

	Natural	Crop	Pasture	Secondary
1500	129.2 (96.4)	2.1 (1.6)	2.7 (2.0)	0.1 (0.1)
1550	124.8 (93.1)	2.2 (1.6)	3.0 (2.2)	4.0 (3.0)
1600	120.9 (90.2)	2.4 (1.8)	3.4 (2.5)	7.4 (5.5)
1650	117.7 (87.8)	2.7 (2.0)	3.6 (2.7)	10.1 (7.5)
1700	115.0 (85.8)	2.9 (2.2)	3.7 (2.8)	12.3 (9.2)
1750	112.1 (83.6)	3.5 (2.6)	4.7 (3.5)	13.9 (10.4)
1800	109.0 (81.3)	4.2 (3.1)	5.7 (4.3)	15.1 (11.3)
1850	104.3 (77.8)	5.7 (4.3)	7.9 (5.9)	16.1 (12.0)

(−3.3% from 1500 to 1550 and −2.9% from 1550 to 1600), mostly because of agricultural expansion.

Under the historical land-use scenario from 1500 to 1850, the area of agricultural lands almost tripled with pastures consistently occupying a larger area than crops. Except for the seventeenth century, pastures have increased at a faster rate than croplands. By 1850, 10.2% of the global natural land area was converted for agriculture use, with 7.9×10^6 km^2 converted to pastures and 5.7×10^6 km^2 converted to croplands. As a result of shifting cultivation and abandonment of agricultural lands, the area of secondary vegetation increased and occupied a larger fraction than agriculture after 1600. Before the start of the nineteenth century, secondary land areas increased at a faster rate than crops and pastures combined such that, by 1850, 12% (16.1×10^6 km^2) of the land surface was covered by the secondary vegetation of various ages.

The regional land-use patterns were analyzed for five continental regions in 1550, 1650, 1750, and 1850 (Figure 2). Before 1850 in North America, there were relatively small changes in land use and secondary vegetation was predominant. Natural vegetation slowly decreased during the entire period (1550–1850) in South America and Europe. Although secondary lands and pastures increased before 1850 in South America, cropland area peaked in 1550 and steadily decreased thereafter until 1850. In 1550, the largest global area occupied by croplands occurred in Europe (10.8% of the region was croplands). Although secondary vegetation and pastures slowly increased during the analysis period in Europe, cropland area increases were significantly larger. By 1850, 20.7% of Europe was covered by croplands.

Natural vegetation decreases in all regions from 1550 to 1850 but is most prominent in Africa, where the largest impact of human activities was experienced between 1550 and 1650 (Figure 2a). Overall, secondary vegetation area is the largest in Africa and dominates land use in this region (almost 30% of the land surface at 1850). Area of pastures rapidly increased between 1750 and 1850 and remained significantly larger than cropland areas. Asia was grouped with Oceania and mainly accounts for the reported regional numbers in this analysis. Only 3% of the land area in Oceania was impacted by land use by 1850. In Asia/Oceania, primary lands were mostly converted to agriculture. Although pasture areas remained larger than cropland areas for all periods, the largest global area of croplands was found in Asia/Oceania (except for 1550).

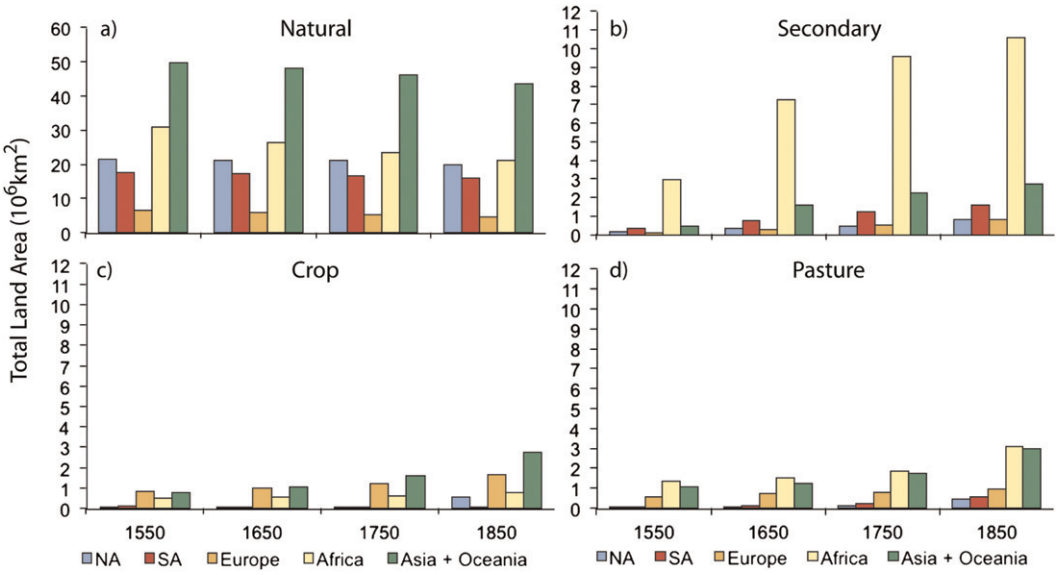

Figure 2. Total land area (10^6 km^2) occupied by (a) natural vegetation; (b) secondary vegetation; (c) crops; and (d) pastures for five regions in 1550, 1650, 1750, and 1850 (Chini et al. 2008).

4.2. Global trends

Averaged over the last 50 years of the 400-yr POTV integration, the simulated global total vegetation and soil carbon were 699.7 (±4.9) and 1604 (±1.1) GtC, respectively, whereas the net carbon flux was 0.07 GtC yr^{-1}, indicating that the POTV integration is near equilibrium. The changes in land carbon in the vegetation and soil pools following historical land-use application is shown in Figure 3 for all scenarios. The large decreasing trend in carbon stores in all land-use curves in Figure 3 is due to anthropogenic lands expansion and the decreasing natural vegetation area. The interannual variability in the vegetation and soil terrestrial carbon stores (as well as the total storage) are tied directly to the atmospheric forcing used in LM3V, the 50 years of climate from the 1860 control CM2.1 experiment. The 50-yr cycle in forcing is evident in the terrestrial carbon pools and demonstrates the sensitivity of the biosphere to climate (Figure 3). Another pronounced feature is the response of the terrestrial biosphere to the simulated ENSO events (Wittenberg et al. 2006). The biases in the CM2.1 climate simulation, such as its exaggerated ENSO cycle and underpredicted precipitation over the Amazonian tropics, result in the increased interannual variability in the global carbon fluxes.

4.3. Carbon response

The overall carbon response to the historical land-use perturbation is similar in all land-use experiments, regardless of when land use was initially applied in the model. In each case, vegetation carbon initially decreased sharply, whereas the soil carbon initially increased because the residue and slash biomass from deforestation

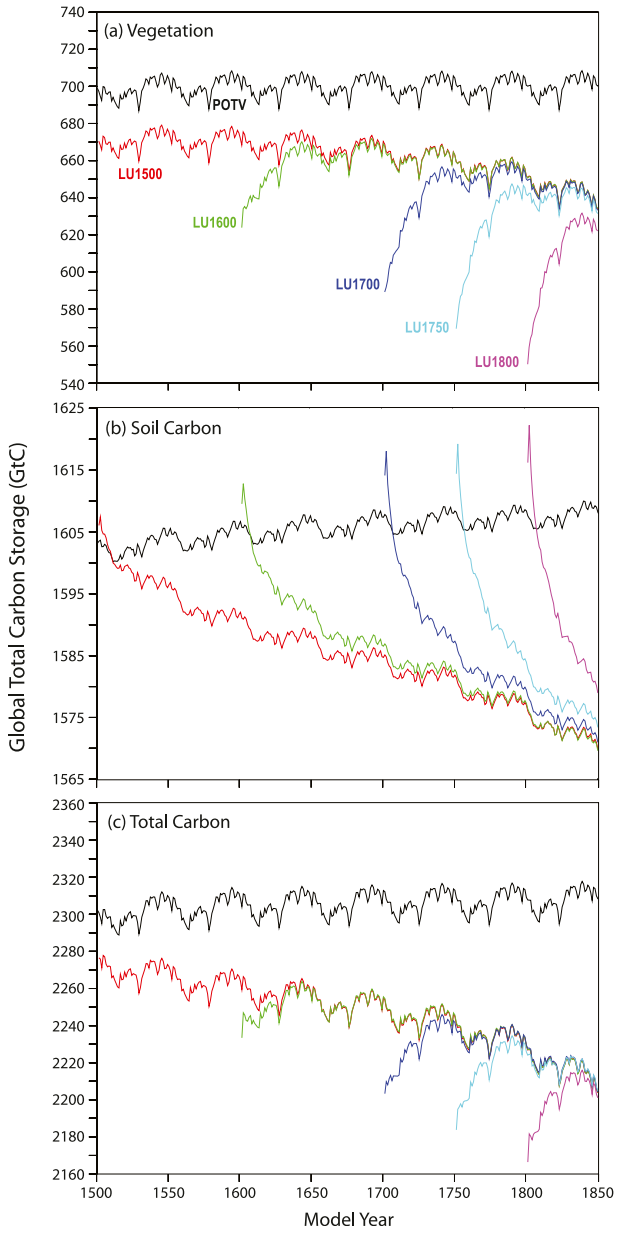

Figure 3. Simulated global (land only) total terrestrial carbon pools for POTV (black), LU1500 (red), LU1600 (green), LU1700 (blue), LU1750 (cyan), and LU1800 (magenta) for (a) vegetation (living and dead biomass); (b) soil organic carbon; and (c) total (vegetation and soil) carbon in GtC.

was deposited from the vegetation pool into the soil pool (Table 2). The abrupt decrease and increase in the vegetation and soil carbon pools, respectively, in year 1 for each land-use experiment are not shown in Figure 3 because they are large relative to the changes resulting from land use in the following years. After that initial response, globally integrated carbon continued to decline throughout the

Table 2. Initial change (GtC) in carbon pools in response to land use applied at different times. Numbers in parentheses indicate initial percent (%) change in carbon pools in response to land use applied at different times.

	Vegetation carbon	Soil carbon	Total carbon
1500	−28.5 (−4.1)	+2.9 (+0.2)	−25.6 (−1.1)
1600	−75.0 (−10.7)	+6.2 (+0.4)	−68.8 (−3.0)
1700	−110.8 (−15.8)	+10.5 (+0.7)	−100.3 (−4.4)
1750	−129.0 (−18.5)	+11.5 (+0.7)	−117.5 (−5.1)
1800	−146.8 (−21.1)	+13.1 (+0.8)	−133.6 (−5.8)

simulation period (Figure 3). The relatively rapid decline in the vegetation carbon during the nineteenth century can be attributed to the increased rate of conversion from natural to agricultural lands during this period. From 1500 to 1850, the land carbon storage decreased by about 98 GtC (i.e., the difference between the 1850 carbon store for LU1500 and the 1500 carbon store for POTV) as a result of land-use activities. Approximately two-thirds of this carbon decrease from 1500 (about 699 GtC from POTV) to 1850 (633.8 GtC from LU1500) comes from the vegetation carbon pool (65.2 GtC) because expanding and regrowing secondary forests stored an increasingly large fraction of carbon. Although all the experiments specify the same area of crops, pastures, and secondary vegetation in 1850, the later land use is applied in the model results in a smaller amount of carbon storage in the secondary forests in 1850. This is because secondary forests in these later experiments have not had enough time to develop mature secondary forests (Figure 3a).

Although the pattern of the carbon responses is similar in all experiments, the magnitude of these responses differs considerably depending on the timing of the scenario application. In the experiments with the historical land-use application later than 1500, one needs first to compute and apply the cumulative transition beginning from 1500 (e.g., from 1500 through 1600 for the LU1600 experiment). Therefore, in most locations, the later the land use is applied to the potential vegetation, the larger the magnitude of the initial transition will be and the more abrupt the change in the carbon stocks will be. For example, the total initial carbon change is larger in 1700 (−100.3 GtC) than in 1500 (−25.6 GtC) (Table 2). As expected, the largest initial total carbon change was in LU1800 with the loss of 133.6 GtC or 5.8% of the total carbon.

As Figure 3 shows, the carbon pools are not at equilibrium at 1850 and continue to decrease because of ongoing land use. To characterize the time scales of response of carbon pools to the timing of the initial, historical land-use application in the context of continued land use, we define a fraction f as

$$f = \frac{\mathrm{Cexp}(t) - \mathrm{Ctarget}(t)}{\mathrm{Cexp}(\tau) - \mathrm{Ctarget}(\tau)}, \tag{1}$$

where Cexp and Ctarget are the global sums (land only) of total (i.e., vegetation and soil) carbon for each land-use experiment (LU1600, LU1700, LU1750, and LU1800) and the target experiment (LU1500) at time t and τ, the year in which we apply land use (i.e., 1600, 1700, 1750, and 1800). Although the magnitude of the initial change in the global vegetation and soil carbon pools differs with the timing of the historical land-use application, the decay rates are similar among the

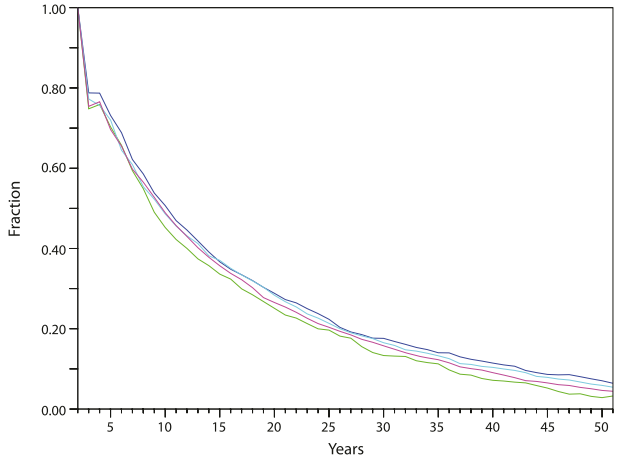

Figure 4. Time plot of the fraction computed using Equation (1) for LU1600 (green), LU1700 (blue), LU1750 (cyan), and LU1800 (magenta) relative to LU1500. The vertical axis is the fraction. The horizontal axis is years from the initial imposition of the historical land-use scenario on POTV.

experiments (Figure 4). This suggests that the time scales of terrestrial carbon response to land use are independent of the timing of land-use application in the model. We found that, after about 80 years from the initial, historical land-use imposition, the global vegetation carbon pool is roughly similar among all land-use experiments. Because most of the global vegetation carbon resides in wood, this time scale is consistent with the recovery time for secondary forests following land-use disturbance. A similar statement can be made for the global soil and total carbon pools after about 150 years.

4.4. Zonal carbon storage after initial land-use application

In addition to our evaluation of global land carbon responses, we also examined the zonally averaged responses in the LU1700 experiment (Figure 5). Zonally averaged responses differ in magnitude from the global response, with the longest response time scales found in the Northern Hemisphere extratropics. In 1700, the largest difference in the vegetation carbon pool from the LU1500 experiment is in the tropics (approximately 0.035 TgC per 2° latitude) followed by the northern midlatitudes (about 0.018 TgC per 2° latitude). The former could be explained by high and rapidly regrowing vegetation biomass in this region compared with other regions. The largest soil carbon difference in 1700 (approximately 0.018 TgC per 2° latitude) is in the northern midlatitudes. The smaller difference in the tropics suggests that, where the soil respiration rates are high and vegetation regrowth is fast, the differences in both soil and vegetation carbon pools are primarily driven by the magnitude of the initial, historical land-use perturbation. In middle to high latitudes, where the soil respiration rates are low, the soil carbon and thus the total pool LU1700 to LU1500 differences are determined by both the extent of land use and time since the initial application of land use. Overall, the global terrestrial

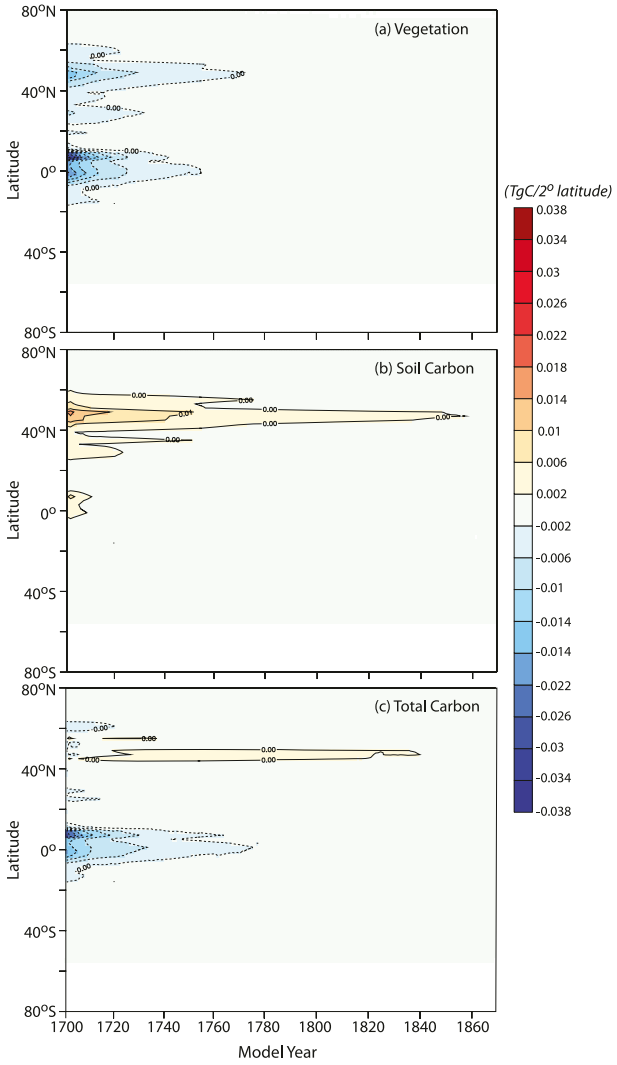

Figure 5. Simulated zonally averaged (land only) total terrestrial carbon pool differences between land use applied at 1700 and 1500 for (a) vegetation (living and dead biomass), (b) soil organic carbon, and (c) total (vegetation and soil carbon) carbon in TgC per 2° latitude.

carbon pool response is made up of two distinct responses: a large deficit in the vegetation carbon pool in the tropics and a surplus in the northern midlatitudes. Even after 160 years, there are some areas in the northern midlatitudes where there are clear differences between the two experiments. However, as shown above, these differences have little impact the global response.

The terrestrial carbon differences between LU1700 and LU1500 in Figure 5 provide information on the time scales of the response to the imposition of land use in each pool. That analysis shows that the differences in the vegetation pool between the LU1700 and LU1500 integrations disappear within approximately 80 years of the imposition of land use. In fact, most of the vegetation carbon (leaves

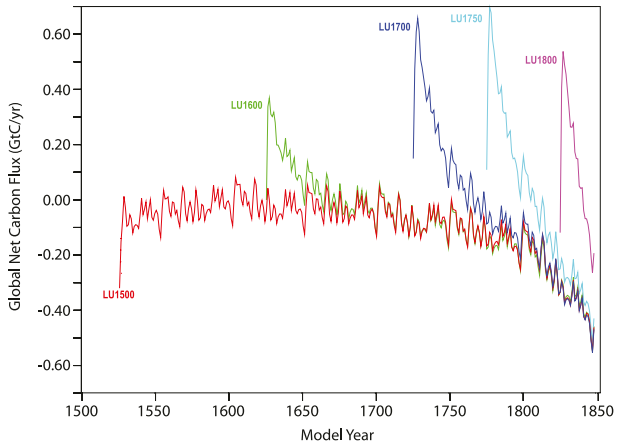

Figure 6. Modeled annual global net carbon flux (GtC yr^{-1}) from LU1500 (red), LU1600 (green), LU1700 (blue), LU1750 (cyan), and LU1800 (magenta). Negative values indicate a terrestrial carbon source, whereas positive values indicate a terrestrial carbon sink.

and roots) responds relatively quickly, within the first 20 years. In contrast to the behavior in the tropics, the response to land use in the midlatitudes is dominated by the storage of carbon in the soil rather than in the vegetation. The soil carbon pools are slower to respond to the imposition of land use, and most of the response is seen within roughly 150 years, whereas the fast soil carbon pools in the tropics and subtropics respond within about 60 years. Because of the increased respiration rates in the tropics, the soil carbon response there is much faster (approximately 10 years) than in the northern midlatitudes (approximately 150 years). The high latitudes (60°–65°N) are predominantly covered by potential vegetation because the land surface has not been altered in these regions as much as in the midlatitudes and tropics. From this analysis, it is clear that, when secondary vegetation is included in ESMs, land use should be applied no later than 1700 to allow both the vegetation and soil pools time to respond to carbon shock imposed by land use in the model. This choice is controlled by the slowest time scale in the terrestrial carbon system, the 150+ year time scale for soil carbon in northern middle latitudes. This yields a good representative initial estimate of the carbon pools at 1860, the start of the GFDL ESM CMIP5 and IPCC AR5 historical experiments

4.5. Net carbon flux after initial land-use application

For our experiments, the initial perturbation resulting from the carbon shock from historical land-use imposition is a sharp, positive net terrestrial carbon flux (Figure 6). This represents the initial flux of carbon into the terrestrial biosphere as the accumulated land use is imposed on the potential vegetation state. Similar to the response in the carbon pools, the magnitude of this perturbation increases the later land use is applied in the model because more of the land surface undergoes instantaneous conversion.

In 1850, the simulated net land carbon sources are 0.418 GtC yr^{-1} for LU1500, 0.412 GtC yr^{-1} for LU1600, 0.427 GtC yr^{-1} for LU1700, 0.390 GtC yr^{-1} for LU1750, and 0.166 GtC yr^{-1} for LU1800 (Figure 6). The 1850 simulated net land carbon source for the LU1500, LU1600, and LU1700 experiments is close to the most recent estimate from Houghton (Houghton 2008), 0.501 GtC yr^{-1}, whereas LU1750 and LU1800 estimates are further from this estimate. This implies that applying initial land use after 1700 in our model is ill advised because it produces nonrealistic values for the land carbon pools and the resulting fluxes because the terrestrial biosphere is still responding to the carbon shock resulting from the initial imposition of the land use.

5. Summary

The terrestrial component of the GFDL ESMs simulates secondary vegetation regrowth following disturbances, such as land conversion to agriculture and forestry. As part of the experiment design for CMIP5 and IPCC AR5, historic simulations of the past (~1850 to present day) are needed. This paper investigates both the technical issues that need to be considered to ensure the terrestrial carbon is as realistic as possible at the start of these integrations and the science questions involving the time scales of the terrestrial carbon response to perturbations.

In our experimental design, we begin with a POTV integration without land use so that potential vegetation and soil carbon are allowed to evolve freely with the climate. This results in an equilibrated carbon state. Any application of land use results in a transient carbon state from 1) time-evolving land-use forcing and 2) the time-evolving response of terrestrial carbon to time-invariant land-use application. The question is, how do we obtain initial conditions for the preindustrial, 1860 terrestrial carbon stores needed at the start of the historical integration? Our solution is to make an additional integration before each historical integration ensemble member in which we impose land use but no other forcings (Figure 1). By imposing land use from a time long before the start of the historical integration, we minimize the impact of "carbon shock," which occurs when land use is applied to the potential vegetation state in the control and also allows time for the secondary forests to regrow. This helps both the soil carbon and the vegetation to find quasi-realistic states at the beginning of the historical integrations. The mechanisms and associated adjustment time scales of response differ for the vegetation and soil carbon pools globally and regionally. The adjustment time scales of the soil carbon pool are much longer than the vegetation and are the main driver in determining how long it takes the total carbon pool to respond to the carbon shock caused by the imposition of land use on the potential vegetation.

Higher soil respiration rates in the tropics (15°S–15°N) allow the soil carbon pools in this area to respond to the carbon shock most rapidly. The northern high-latitude (north of 60°N) carbon pools are not as impacted by the land-use changes before 1850 because there are only small areas of land use before this time. When looking at the impact on the global adjustment time scale, the reduced soil respiration rates in the northern midlatitudes (30°–60°N) are the main factor setting the time scale for the globally averaged soil carbon.

We found that, in approximately 150 years following the initial, historical land-use application, the terrestrial carbon stores and fluxes resemble those where land

use was applied much earlier in the integration. Because our historical integration starts in 1860, this means we will start imposing land use from the year 1700. We found that initializing land use in 1700 results in a simulated net land carbon flux to the atmosphere in 1850 in good agreement with a recent estimate using a bookkeeping approach (Houghton 2008). We thus recommend the initialization of land use in 1700 in the GFDL ESMs as a computationally efficient technique for ensuring that the terrestrial carbon is realistic at the start of the historical simulations in 1860. This recommendation saves 200 model years of integration relative to starting historical land-use transitions in 1500, saving us about 20 days of integration on our present computer system.

Although the focus of this paper is on the terrestrial carbon response to the application of global land-use change, several interesting science questions can be explored using regional land-use datasets, such as Steyaert and Knox (Steyaert and Knox 2008) and Hurtt et al. (Hurtt et al. 2002). The availability of different regional land-use datasets enables future studies on the impacts of regional land use on terrestrial carbon and the interactions and feedbacks with climate.

Acknowledgments. We wish to thank George Hurtt and Louise Parsons Chini for providing us with the historical land-use transition datasets. We also thank John Dunne, Kirsten Findell, and Larry Horowitz for reviewing earlier versions of this manuscript and Cathy Raphael for producing the illustration figures.

References

Bolker, B. M., S. W. Pacala, and W. J. Parton, Jr., 1998: Linear analysis of soil decomposition: Insights from the century model. *Ecol. Appl.,* **8,** 425–439, doi:10.1890/1051-0761(1998)008[0425:LAOSDI]2.0.CO;2.

Canadell, J. C., M. Kirschbaum, W. Kurz, M.-J. Sanz, B. Schlamadinger, and Y. Yamagata, 2007: Factoring out natural and indirect human effects on terrestrial carbon sources and sinks. *Environ. Sci. Policy,* **10,** 370–384.

Chini, L. P., and Coauthors, 2008: Harmonization of global land-use scenarios for the period 1500-2100 for IPCC 5th Assessment. *Eos Trans. Amer. Geophys. Union,* **89** (Fall Meeting Suppl.), Abstract B41B-0378.

DeFries, R. S., L. Bounoua, and G. J. Collatz, 2002: Human modification of the landscape and surface climate in the next fifty years. *Global Change Biol.,* **8,** 438–458.

Delworth, T. L., and Coauthors, 2006: GFDL's CM2 global coupled climate models. Part I: Formulation and simulation characteristics. *J. Climate,* **19,** 643–674.

Denman, K. L., and Coauthors, 2007: Couplings between changes in the climate system and biogeochemistry. *Climate Change 2007: The Physical Science Basis,* S. Solomon et al., Eds., Cambridge University Press, 499–587.

Hoffman, F., I. Fung, and J. John, 2005: Preliminary results from the C4MIP phase 1 simulations using the CCSM3-CLM3-CASA coupled model. *Eos, Trans. Amer. Geophys. Union,* **86** (Fall Meeting Suppl.), Abstract B33G-07.

Houghton, R. A., 1999: The annual net flux of carbon to the atmosphere from changes in land use 1850-1990. *Tellus,* **51B,** 298–313.

——, 2003: Revised estimates of the annual net flux of carbon to the atmosphere from changes in land use and land management 1850–2000. *Tellus,* **55B,** 378–390.

——, 2008: Carbon flux to the atmosphere from land-use changes: 1850-2005. TRENDS: A compendium of data on global change, U.S. Department of Energy Oak Ridge National Laboratory Carbon Dioxide Information Analysis Center Rep.

Hurtt, G. C., S. W. Pacala, P. R. Moorcroft, J. Caspersen, E. Shevliakova, R. A. Houghton, and Moore B. III, 2002: Projecting the future of the U.S. carbon sink. *Proc. Natl. Acad. Sci. USA,* **99,** 1389–1394.

——, S. Frolking, M. G. Fearon, B. Moore, E. Shevliakova, S. Malyshev, S. W. Pacala, and R. A. Houghton, 2006: The underpinnings of land-use history: Three centuries of global gridded land-use transitions, wood-harvest activity, and resulting secondary lands. *Global Change Biol.,* **12,** 1208–1229, doi:10.1111/j.1365-2486.2006.01150.x.

Jain, A. K., and X. Yang, 2005: Modeling the effects of two different land cover change data sets on the carbon stocks of plants and soils in concert with CO_2 and climate change. *Global Biogeochem. Cycles,* **19,** GB2015, doi:10.1029/2004GB002349.

Kucharik, C. J., and Coauthors, 2000: Testing the performance of a dynamic global ecosystem model: Water balance, carbon balance, and vegetation structure. *Global Biogeochem. Cycles,* **14,** 795–825.

McGuire, A. D., and Coauthors, 2001: Carbon balance of the terrestrial biosphere in the twentieth century: Analyses of CO_2, climate and land use effects with four process-based ecosystem models. *Global Biogeochem. Cycles,* **15,** 183–206.

Pacala, S. W., and Coauthors, 2001: Consistent land- and atmosphere-based U.S. carbon sink estimates. *Science,* **292,** 2316–2320.

Pongratz, J., C. H. Reick, T. Raddatz, and M. Claussen, 2009: Effects of anthropogenic land cover change on the carbon cycle of the last millennium. *Global Biogeochem. Cycles,* **23,** GB4001, doi:10.1029/2009GB003488.

Randall, D. A., and Coauthors, 2007: Climate models and their evaluation. *Climate Change 2007: The Physical Science Basis,* S. Solomon et al., Eds., Cambridge University Press, 589–662.

Shevliakova, E., and Coauthors, 2009: Carbon cycling under 300 years of land-use change: The importance of the secondary vegetation sink. *Global Biogeochem. Cycles,* **23,** GB2022, doi:10.1029/2007GB003176.

Steyaert, L. T., and R. G. Knox, 2008: Reconstructed historical land cover and biophysical parameters for studies of land-atmosphere interactions within the eastern United States. *J. Geophys. Res.,* **113,** D02101, doi:10.1029/2006JD008277.

Taylor, K. E., R. J. Stouffer, and G. A. Meehl, 2011: An overview of the CMIP5 and the experiment design. *Bull. Amer. Meteor. Soc.,* submitted.

Wittenberg, A. T., A. Rosati, N.-C. Lau, and J. J. Ploshay, 2006: GFDL's CM2 global coupled climate models. Part III: Tropical Pacific climate and ENSO. *J. Climate,* **19,** 698–722.